https://doi.org/10.5194/egusphere-2023-521
Preprint. Discussion started: 24 March 2023

Assessment of the impacts of cloud chemistry on surface SO_2 and sulfate levels in typical regions of China

Jianyan Lu[1], Sunling Gong[1,5]*, Jian Zhang[1], Jianmin Chen[2,3,4], Lei Zhang[1], Chunhong Zhou[1]*

[1] State Key Laboratory of Severe Weather, Key Laboratory of Atmospheric Chemistry of CMA, Institute of Atmospheric Composition, Chinese Academy of Meteorological Sciences, Beijing 100081, China
[2] Shanghai Key Laboratory of Atmospheric Particle Pollution and Prevention (LAP3), Department of Environmental Science and Engineering, Fudan Tyndall Centre, Institute of Atmospheric Sciences, Fudan University, Shanghai, China
[3] Center for Excellence in Urban Atmospheric Environment, Institute of Urban Environment, Chinese Academy of Science, Xiamen, China
[4] Shanghai Institute of Eco-Chongming (SIEC), No.3663 Northern Zhongshan Road, Shanghai 200062, China
[5] National Observation and Research Station of Coastal Ecological Environments in Macao, Macao Environmental Research Institute, Macau University of Science and Technology, Macao SAR 999078, China

* Corresponding authors.

E-mail addresses: gongsl@cma.gov.cn (S. Gong), zhouch@cma.gov.cn (C. Zhou)

Abstract

A regional online chemical weather model WRF/ CUACE (China Meteorological Administration Unified Atmospheric Chemistry Environment) is used to assess the contributions of cloud chemistry to the SO_2 and sulfate levels in typical regions in China. By comparing with several time series of in-situ cloud chemical observations on Mountain Tai in Shandong Province of China, the CUACE cloud chemistry scheme is found to well reproduce the cloud processing the consumption of H_2O_2, O_3 and SO_2 and the increase of sulfate, and consequently is used in the regional assessment for a heavy pollution episode and monthly average in December 2016. During cloud availability in heavy pollution episode, the sulfate production increases 60-95% and SO_2 reduces over 80%. And the cloud chemistry mainly affects the middle and lower troposphere below 5 km as well as within the boundary layer, and contributes significantly to SO_2 reduction and sulfate increase in east-central China. Among the four typical contaminated regions in China, the Sichuan Basin (SCB) is mostly affected by the cloud chemistry, with the average SO_2 abatement about 1-15 ppb and sulfate increase about 10-70 μg/m^3, followed by Yangtze River Delta (YRD) where SO_2 abatement is about 1-3 ppb and sulfate increase is about 10-30 μg/m^3. However, the cloud chemistry contribution to Pearl River Delta (PRD) and North China Plain (NCP) are not significant and weaker than other two regions due to lighter pollution and less water vapor, respectively. In addition, the average contribution of cloud chemistry during the pollution period is distinctly greater than that for all December. This study provides a way to analyze the

https://doi.org/10.5194/egusphere-2023-521
Preprint. Discussion started: 24 March 2023

over-estimate phenomenon of SO_2 in many chemical transport models.

Keywords: SO_2, sulfate, cloud chemistry, WRF/CUACE

1 Introduction

Aerosols interact with radiation and clouds, directly or indirectly affecting the atmospheric radiation balance and precipitation, which in turn affects weather and climate (Twomey et al., 1984; Twomey, 1991; Charlson et al., 1992; Ramanathan et al., 2001; Pye et al., 2020) . Moreover, large amounts of aerosols dispersed in the atmosphere can reduce visibility and deteriorate air quality (Molina, 2002), which is harmful to human health and ecosystem (Xie et al., 2019; Sielski et al., 2021).

In addition to direct emissions, aerosols are mostly produced secondarily through the oxidation of precursor gases, and one of the important processes is the transformation in clouds. Global cloud coverage of about 21% to 95% provides an adequate environment for cloud chemistry processes (Kotarba, 2020; Ravishankara, 1997). As about 90% of the clouds formed in the atmosphere evaporate without deposition or forming the precipitation, large fractions of aerosols formed in them can then re-enter the atmosphere (Caffrey et al., 2001; Harris et al., 2013; Lelieveld et al., 1992). Globally, sulfate production from SO_2 oxidation accounts for about 80% of total sulfate, and more than half of it is produced in clouds (Hung et al., 2018; Faloona et al., 2010; Guo et al., 2012). Ge et al. (2021) found that cloud chemistry processes reduced SO_2 concentrations by 0 ~ 50% in most of east-central China in all seasons. Li (2011) found that the average SO_4^{2-} concentration in cloud water accounted for 53.8% of the total aerosol concentration at a Mount site. Li et al. (2020) also found that cloud processes effectively reduced atmospheric O_3 and SO_2 concentrations by an average of 19.7% and 71.2%, respectively, at Mount Tai.

Multiphase oxidation of sulfate aerosols from SO_2 in aerosol particles in high humidity environment is one of the main causes of explosive growth of particulate matter in East Asia haze (Guo et al., 2014; Cheng et al., 2016; Song et al., 2019). From observations and laboratory works, there are four main pathways for this kind of oxidation of SO_2 which are H_2O_2, O_3, NO_2, and transition metal ions (TMIs) ((IIbusuki and Takeuchi, 1987; Martin et al., 1991; Alexander et al, 2009; Harris et al., 2013; Cheng et al., 2016; Wang et al., 2016). Additional pathways of organic peroxides (ROOH) (Yao et al., 2019; Wang et al., 2019; Ye et al., 2018; Dovrou et al., 2019, photolysis products of nitrate (pNO_3^-) (Gen et al., 2019a; 2019b), and excited triplet states of photosensitizer molecules (T*) (Wang et al., 2020) have also been found recently to be important for multiphase oxidation of sulfur dioxide during very heavy hazy days. Unfortunately there are still much uncertainties and gaps

https://doi.org/10.5194/egusphere-2023-521
Preprint. Discussion started: 24 March 2023

to put all of those pathways into model applications from observational and laboratory studies (Pye et al., 2020; Ravishankara, 1997; Liu et al., 2021). Several regional and global models have tried to include only two, O_3 and H_2O_2, in-cloud oxidant in cloud chemistry mechanisms (Park et al., 2004; Tie et al., 2005; Salzen et al., 2000; Chapman et al., 2009; Leighton and Ivanova, 2008). A very few models can simulate the pathway of NO_2, TMIs of Fe or Mn ions (Ge et al., 2021; Binkowski and Roselle, 2003; Chang et al., 1987; Terrenoire et al., 2015; Menut et al., 2013).

There has been very serious air pollution in central-east China where four heavy pollution zones of North China Plain (NCP), Yangtze River Delta (YRD), Sichuan Basin (SCB) and Pearl River Delta (PRD) are located (Yao et al., 2021; Zhang et al., 2012). Although many global and regional models have contained sulfate formation mechanisms in cloud chemistry, few models have assessed its contribution, especially the lack of detailed assessment of regional cloud chemistry on sulfate and SO_2 in China and those four typical pollution regions. Regional chemical models have reported the over-estimate of SO_2 (Buchard et al., 2014; He et al., 2015; Wei et al., 2019; Sha et al., 2019; Georgiou et al., 2018). The inadequate inclusion or lack of cloud chemistry of SO_2 consumption simulations is one of the main causes (Ge et al., 2021). Therefore, there is a very important need to quantify the contribution of cloud chemistry in these typical regions in central-east China when it comes to heavily polluted weather to get a better understand of multi-dimensional pollution interactions, especially between the upper layer and the surface.

This study is intended to use an on-line coupled chemical weather platform of CMA, WRF/CUACE, to analyze and evaluate the SO_2 in-cloud oxidation process in the four pollution regions in China, with two objectives: (1) evaluating the cloud chemistry scheme in WRF/CUACE by the in-situ cloud chemistry observations at Mount Tai in summers of 2015 and 2018; and (2) quantifying the contributions of cloud chemistry to the SO_2 and sulfate changes in a typical winter pollution month of December 2016 with a very long lasting heavy pollution episode. It is aimed to establish a system to assess the relative contribution of cloud chemistry to SO_2 oxidation pathways and sulfate productions to other clear-sky processes.

2 Model description and Methodology

2.1 Cloud chemistry in WRF/CUACE

WRF/CUACE is an on-line coupled chemical transport model under the WRF frame work with a comprehensive chemical module - CUACE, which is developed at CMA with a sectional aerosol physics, gas chemistry, aerosol-cloud interactions and thermodynamic equilibrium (Zhou et al., 2012; Zhou et al., 2016; Gong et al., 2003; Gong and Zhang, 2008; Zhang et al., 2021). There are seven types of aerosols, i.e. black carbon, organic carbon, sulfate, nitrate, ammonium, soil dust, and sea salt, and more than 60 gaseous species. The aerosol size spectrum is divided into 12 bins with fixed boundaries of

https://doi.org/10.5194/egusphere-2023-521
Preprint. Discussion started: 24 March 2023

0.005-0.01, 0.01-0.02, 0.02-0.04, 0.04-0.08, 0.08-0.16, 0.16-0.32, 0.32-0.64, 0.64-1.28, 1.28-2.56, 2.56-5.12, 5.12-10.24 and 10.24-20.48 μm. The system can simulate PM_{10}, $PM_{2.5}$, O_3 and visibility. A complete heterogeneous chemistry module has been built in CUAC for nine gas-to-particle heterogeneous reactions including SO_2 to sulfate in CUACE (Zhou et al., 2021, Zhang et al., 2021). The cloud chemistry mechanism in CUACE considers the pathways of multiphase oxidation of SO_2 by H_2O_2 and O_3 in both stratocumulus and convective clouds (Gong et al., 2003; Von Salzen et al., 2000). The transport and chemical effects of sulfur in convective clouds are calculated based on a convective cloud model by WRF. Within the cloudy part of a grid box, the first-order rate constant (in s^{-1}) of S(IV) oxidation is given by the following expression:

$$F = \left| \frac{1}{C_{S(IV)}} \frac{\mathrm{d}C_{S(IV)}}{dt} \right| = F_1 C_{O_3} + F_2 C_{H_2O_2} \quad (1)$$

where $C_{S(IV)}$ is the total concentration of S(IV) (gas phase plus dissolved), C_{O_3} is the total concentration of O_3, and $C_{H_2O_2}$ is the total concentration of hydrogen peroxide.

The effective rate constants F_1 and F_2 are given by the following expressions:

$$F_1 = R_{O_3} f_1 \quad (2)$$

$$F_2 = R_{H_2O_2} f_2 \quad (3)$$

The reaction rate constants R_{O_3} and $R_{H_2O_2}$ refer to Maahs (1983) and Martin et al. (1984):

$$R_{O_3} = \left\{ 4.4\times10^{11} \exp(-4131/T) + 2.61\times10^{3} \exp(-966/T) \left[H^+\right]^{-1} \right\} (Ms)^{-1} \quad (4)$$

$$R_{H_2O_2} = 8\times10^{4} \exp\left[-3650(1/T - 1/298)\right] \left\{ 0.1 + \left[H^+\right] \right\}^{-1} (Ms)^{-1} \quad (5)$$

In Equations (2) and (3), the factors f_1 and f_2 represent the partitioning of the substance between the aqueous and gas phases and are determined by the Henry's law coefficients.

$$f_1 = \gamma f_{SO_2} f_{O_3} K_S \overline{K}_{HO} \quad (6)$$

$$f_2 = \gamma f_{SO_2} f_{H_2O_2} \overline{K}_{HS} \overline{K}_{HP} \quad (7)$$

where γ is the dimensionless volume fraction of liquid water in the cloud. The parameters f_{SO_2}, f_{O_3} and $f_{H_2O_2}$ are the proportions of individual substances in the gas phase. They are also calculated from the dimensionless Henry's law constant and γ.

$$f_{SO_2} = \left(1 + \gamma \overline{K}_{HS} K_S\right)^{-1} \quad (8)$$

https://doi.org/10.5194/egusphere-2023-521
Preprint. Discussion started: 24 March 2023

$$f_{O_3} = \left(1 + \gamma \overline{K}_{HO}\right)^{-1} \quad (9)$$

$$f_{H_2O_2} = \left(1 + \gamma \overline{K}_{HP}\right)^{-1} \quad (10)$$

With

$$K_S = \overline{K}_{HS}\left(1 + \frac{K_{1S}}{[H^+]} + \frac{K_{1S}K_{2S}}{[H^+]^2}\right) \quad (11)$$

The Henry's law constants used in (6) to (8) are listed in table 1. The equilibrium constant K_{HS} in Table 1 is set to be 1.23×10^{-3} M/atm in CUACE which is the same to that in Von et al (2000) but is 10^3 times lower than that in Leighton et al (1990).

In order to consider the dependence of the oxidation rates on the pH, the H^+ concentration is calculated from ions balance.

$$[H^+] + [NH_4^+] = [OH^-] + 2[SO_4^{2-}] + 2[SO_3^{2-}] + [HSO_3^-] + [NO_3^-] + [HCO_3^-] \quad (12)$$

From Eqs. (1) ~ (12), CUACE can simulate the oxidation rates of SO_2 by H_2O_2 and O_3 mainly in the liquid and gaseous environment in both stratocumulus and convective clouds in three-dimensional way.

2.2 Assessment criteria

Three variables, RTCLD, DT, and RT, are defined to assess the effect of the cloud chemistry mechanism on SO_2 and sulfate. The RTCLD is defined as the ratio of changes in chemical species concentrations with and without the cloud chemistry mechanism.

$$RTCLD(i) = 1 - \frac{BECLD(i)}{AFCLD(i)} \quad (13)$$

Where i denotes the chemical component of SO_2, O_3, H_2O_2, and sulfate, hereafter. The BECLD denotes the concentration of component i before cloud chemistry, and the AFCLD after the cloud chemistry.

The DT indicates the difference in concentration of substance i with (CLD) and without (CCLD) cloud chemistry.

$$DT(i) = CLD(i) - CCLD(i) \quad (14)$$

The RT represents the concentration ratio change of the substance i with and without cloud chemistry:

$$RT(i) = 1 - \frac{CCLD(i)}{CLD(i)} \quad (15)$$

https://doi.org/10.5194/egusphere-2023-521
Preprint. Discussion started: 24 March 2023

2.3 Methodology

2.3.1 Model Evaluation – Case 1

Mount Tai with an altitude of about 1500 m, located in central Shandong Province, is the high point of the North China Plain. As the Riguan Peak of Mount Tai is far from pollution sources, and the water vapor conditions in summer favors very much cloud formations, it is an ideal observation site for cloud chemistry observation (Li et al., 2017; Li et al., 2020a; Li et al., 2020b). The observed concentrations of SO_2, O_3 and H_2O_2 in cloudy conditions from June 19 to July 30, 2015 and from June 20 to July 30, 2018 with time interval of 1 h are obtained to evaluate the cloud chemistry scheme in WRF/CUACE (Li et al., 2017; Li et al., 2020a; Li et al., 2020b).

WRF/CUACE is set up with two-domain nesting for the evaluation, with the Riguan Peak as the central point (Fig. 1a). The horizontal resolution of outer domain (O) is 9 km with 100×104, and of the inner domain (I) is 3 km with 88×94 (Fig. 1a). There are 32 vertical layers with the top pressure of 100 hPa.

2.3.2 Simulations of Regional Characteristics – Case 2

In order to assess the regional contribution of cloud chemistry to SO_2 and sulfate in CUACE, December 2016 is selected with a widespread heavy pollution episode occurred in North and East China from Dec. 16 to 21 and covering NCP, YRD and SCB with the highest hourly fine particulate matter ($PM_{2.5}$) concentration exceeding 1100 μg m^{-3} (Yuan and Ma, 2017). The simulation region is set up as shown in Figure1b also with two-level domain nesting. The outer domain (O) covers Central and East Asia with a horizontal resolution of 54 km and a grid of 139×112. The inner domain (I) covers most of China on the eastern side of the Qinghai-Tibet Plateau with a horizontal resolution of 18 km and a grid of 157×166. The vertical layer number of the model is the same as that in the Case 1.

Since the cloud water is the reaction pool of cloud chemistry, whether the simulation of cloud water is reasonable or not is directly related to the effectiveness of cloud chemistry. Both the cloud water and rainwater from WRF are coupled to the cloud chemistry module and main physics configurations are listed in Table 2.

2.4 Meteorological, environmental and Satellite Data

For both cases, the meteorological initial and boundary conditions for WRF/CUACE are from NCEP (National Centers for Environmental Prediction) FNL global reanalysis at a resolution of 1° with 6-h interval. The chemical lateral boundary conditions are from NOAA (National Oceanic and Atmospheric Administration) Meteorological Laboratory Regional Oxidant Model (NALROM) (Liu et al., 1996). The model is run in a restart way with a 5-day spin-up.

https://doi.org/10.5194/egusphere-2023-521
Preprint. Discussion started: 24 March 2023

FY-2G cloud image data of CMA (China Meteorological Administration) with an 1 h interval is used to evaluate the cloud in both cases. Routine observations in 3 h interval from 23 meteorological stations of CMA and hourly pollution observations from 132 stations of the China General Environmental Monitoring Station are used to evaluate the meteorological fields and pollutants for December 2016. This includes Beijing, Tianjin, Tangshan, Shijiazhuang, Baoding, Hengshui and Jinan in the North China Plain, Shanghai, Nanjing, Hangzhou, Hefei, Suzhou, Yangzhou and Nantong in the Yangtze River Delta, Guangzhou, Dongguan, Zhuhai and Zhongshan in the Pearl River Delta, and Chengdu, Yibin, Nanchong, Deyang and Zigong in the Sichuan Basin. Meteorological elements include 2 m air temperature, 2 m relative humidity, and 10 m wind speed.

The MEIC (Multi-resolution Emission Inventory for China) inventory, at a resolution of 0.25˚, is used as the anthropogenic emissions with the species of sulfur dioxide (SO_2), nitrogen oxides (NO_x), carbon monoxide (CO), ammonia (NH_3), black carbon (BC), organic carbon (OC), non-methane volatile organic compounds (NMVOCs), $PM_{2.5}$ and PM_{10} by five sectors of power, industry, transportation, residential, and agriculture (Li et al.,2017; Zheng et al.,2018). The emission base year of 2015 and 2017 are used for Case-1, of 2016 for Case-2, respectively.

3 Results and Discussions

3.1 Evaluation of the cloud chemistry mechanism

In order to verify the cloud chemistry mechanism in WRF/CUACE, the simulations are compared with the observations at Mount Tai. By analyzing the satellite cloud images in and around Mount Tai and matching with the available observed data, two time periods with clouds from June 19 to July 30, 2015 and June 20 to July 30, 2018 are selected for the comparisons, defined as "cloud process-1" (CP-1) and "cloud process-2" (CP-2), respectively. The statistics of correlation coefficients (R), relative average deviation (RAD), and normalized mean deviation (NMB) between hourly simulated and observed SO_2, O_3, H_2O_2 and sulfate are shown in Table 3. The results show that the RADs of SO_2, O_3, H_2O_2 and sulfate in CP-1 and CP-2 are in the range of -35 % ~ 78 %, and the R for the four species are 0.34, 0.33 and 0.61 and 0.32 for CP-1, and 0.47, 0.40, 0.06 and 0.54 for CP-2, respectively. The simulated and observed averages are within the same magnitude and close to each other. Among them, the simulated and observed averages of SO_2 are very close in both CP-1 and CP-2, with RAD about -3% and -6%. The analysis reveals that although the correlation of H_2O_2 in CP-2 is only 0.06, the RAD is 18%, the NMB is -19.6%, and the simulated mean value of H_2O_2 is closer to the observed mean value compared to CP-1. For sulfate, the simulated correlation is good with R of 0.32 and 0.54, but the model underestimates sulfate concentrations with NMB of -71 % and -59.4 %. This indicates that although the model is able to simulate the trend of sulfate concentrations, the simulated

https://doi.org/10.5194/egusphere-2023-521
Preprint. Discussion started: 24 March 2023

concentrations are lower than the observed values. Therefore, the underestimation of sulfate may be due to the incompleteness of other cloud chemistry mechanisms or the bias of liquid water content in the cloud physics. The above results show that SO_2, sulfate, and two important oxidants, O_3 and H_2O_2, are reasonably simulated in both time periods.

It is also found that when cloud chemistry occurs, SO_2 concentration values range from 0-2.5 ppbv, mostly less than 1 ppbv in CP-2, O_3 in the range of 25-125 ppbv, H_2O_2 in the range of 0-100 μM (Fig. 2), and sulfate in the range of 0-100 μg/m^3. All four species are agreed within a factor two of observed concentrations, while the sulfate is obvious underestimated in CP-1. In addition, CP-2 shows the observed concentration of H_2O_2 is increased, compared to CP-1. The SO_2 concentrations are small for both time periods. Shen et al. (2012) found mean SO_2 concentrations of 8.1 ppbv and 6.4 ppbv for the Mount Tai site in summer 2007 and 2008. Li et al. (2020) observed that the yearly mean summer SO_2 concentrations of 1.3 ± 1.1 ppbv, 0.3 ± 0.2 ppbv, and 0.4 ± 0.2 ppbv in 2014, 2015, and 2018, respectively. The average O_3 concentrations are 50.3 ± 10.9 ppbv, 73.1 ± 19.7 ppbv and 66.3 ± 18.3 ppbv, respectively. The mean H_2O_2 concentrations are 11.6 ± 13.1 μM, 22.8 ± 13.1 μM, and 45.1 ± 29.5 μM, respectively. Besides, H_2O_2 concentrations are 0.55 ± 0.67 ppbv in 2007 (Ren et al., 2009), 0.93 ± 1.01 ppbv in 2018 (Ye et al., 2021), 2.05 ± 1.20 ppbv in 2019 (Ye et al., 2021). The results of our simulations are consistent with the trends of other observational studies, which all indicate clearly cloud chemistry processes consume SO_2, H_2O_2 and O_3 to produce sulfate. The results of our simulations are consistent with the trends of other observational studies, which all indicate clearly an increase in the atmospheric oxidation and a decrease in the SO_2 concentration.

Figure 3 shows the satellite cloud images, simulated column cloud and simulated liquid water content at 8:00 LST on June 24, and 8:00 LST on June 25 in CP-1. The results indicate that not only the simulated column cloud but also the cloud liquid water distribution simulated at the two times are consistent with the satellite observations.

Figure 4 shows the RTCLD of SO_2 and simulated liquid water contents at 2:00 and 8:00 LST on June 24, and 2:00 and 8:00 LST on June 25 in CP-1. The results indicate that the RTCLD of SO_2 distribution simulated at the four times are consistent with the cloud liquid water, so for the distribution of RTCLD of SO_2 with a reduction of more than 80% within the cloud region of Mount Tai and most of Shandong province, which is consistent with the cloud chemistry observation studies by Li (2020).

In summary, the cloud chemistry mechanism in WRF/CUACE is reasonable to reproduce the cloud chemistry for the gaseous pollutant SO_2, sulfate and the important oxidants of O_3 and H_2O_2. The model not only simulates the concentrations of the four species, but also the SO_2 decreasing trend and O_3 and H_2O_2 increasing trends with year.

https://doi.org/10.5194/egusphere-2023-521
Preprint. Discussion started: 24 March 2023

3.2 Assessment of the cloud chemistry impacts on regional SO_2 and sulfate

This session will further assess the contribution of cloud chemistry for the four main pollution regions of NCP, YRD, PRD, and SCB (Fig. 1) in China for the whole December of 2016 and a pollution episode occurred during this period (Dec. 16-21) as Case 2.

3.2.1 Meteorological evaluation

As the driving force of air pollution and cloud chemistry, the meteorological conditions simulated in the four major pollution regions (Table 4) are evaluated with observations. The correlations of all elements with observations are very close in both the whole December and the heavy pollution in four regions, indicating that the model performed well both in December and the heavy pollution episode. The temperature correlation is the best in December, followed by humidity and then wind speed which is consistent with previous researches (Zhou et al., 2012; Wang et al., 2015; Gao et al., 2016). The RMSEs of wind speeds all range from 1.03 to 1.50 m s^{-1}, falling within the criteria (less than 2 m s^{-1}) to define "good" model performance in stagnant weather proposed by Emery et al. (Emery et al., 2001). The RSME of wind speed during heavy pollution is smaller than that of December, which indicates that the model can well performance the static wind even though it is very small.

Figure 5 shows the satellite cloud image, simulated column cloud and simulated liquid water content for the maturation and dissipation stages of the episode. The satellite image shows that the cloud coverage region is mainly in the southwest including SCB on the 19th, almost covers most of eastern China including NCP, YRD, PRD and SCB on the 20th and the 21st, and then move eastward outside of China on the 22nd (Fig.4 a1-d1). The simulated clouds fit well with the satellite images (Fig.4 a2-d2). Since the cloud chemistry occurs in the cloud area, the cloud chemistry mainly affects three regions of NCP, YRD and SCB of the four pollution regions as PRD has relatively much less cloud. The column liquid water distribution also moves from west to east as the episode develops (Fig.5 a3-d3), but is located more southern part of eastern China than that of the cloud. In SCB and YRD, there is more abundant in liquid water content, which can reach more than 500 g m^{-2}, while in PRD There is slightly less, up to 100 g m^{-2}, and in NCP there is the least liquid water content, 0.1 g m^{-2} mostly due to the dry environment and partly due to the overestimated temperature and underestimated humidity in Table 4.

The above analysis shows that the model basically reproduces the meteorological field in December and heavy pollution periods, which provides a better meteorological background basis for the effective simulation of pollution as well as cloud chemistry.

https://doi.org/10.5194/egusphere-2023-521
Preprint. Discussion started: 24 March 2023

3.2.2 Pollutants Evaluation

The simulated hourly $PM_{2.5}$, O_3 and SO_2 concentrations in four regions are also compared with the observations (Table 5). The simulations are all within a factor of two of the observations (figure omitted), and the mean values of the three pollutants simulated in the four regions are very close to the observations, indicating that model captures well the variability of $PM_{2.5}$, O_3 and SO_2 concentrations during both December 2016 and the heavy pollution episode. In detail, O_3 correlates well with observations in all four regions for the whole month but not so well in the episode. $PM_{2.5}$ correlates better at PRD and YRD during the episode, but not so well in other regions and other two time periods. It is much less underestimated at NCP and SCB. Compared to the whole month, SO_2 is better simulated at NCP, YRD, and SCB during the pollution period. The following part of this paper will focus on assessing the effects of cloud chemical processes.

3.2.3 Assessment of regional contributions

The regional impacts of cloud chemical processes on surface SO_2 and sulfate are analyzed for whole December and for a pollution episode of Dec. 16-21. The pollution episode is investigated with respect to the maturity stage (21:00 LST on Dec. 20 - 17:00 LST on Dec. 21) and to the dissipation stage (2:00 LST on Dec. 22) for the four pollution regions NCP, YRD, PRD, and SCB.

The average impact of cloud chemistry on surface SO_2 and sulfate in December (Fig. 6, DT(SO_2) and DT (sulfate)) is simulated. It is found that SO_2 declination in December is concentrated mostly in the central-eastern part of China, by an average of 0.1-1 ppb in most regions. SO_2 concentrations are reduced by 0.5-3.0 ppb in most part of NCP, YRD, PRD and SCB regions. Among them, there is a relatively stronger center by declining 3.0-10.0 ppb in SCB. Correspondingly, sulfate growth is mainly centering in SCB, with the maximum center up to 20-50 $\mu g/m^3$. Sulfate concentrations are increased by 10-20 $\mu g/m^3$ in most part of NCP, YRDand PRD, and increased 5-10 $\mu g/m^3$ in others.

The spatial distribution of cloud chemistry contribution to SO_2 and sulfate during the whole mature stage of the heavy pollution is analyzed (Fig. 7, DT(SO_2) and DT(sulfate)) on the 19th to the 21st. It shows that SO_2 decreases most significantly in SCB, exceeding 1-3 ppb in most area, to 3-10 ppb in the central region. It also reaches 1-3 ppb in most parts of YRD, PRD and NCP, while the smallest decrease is below 1 ppb in the northern part of NCP. Meanwhile, in terms of regional distribution, the regions of increasing sulfate concentration and decreasing sulfur dioxide concentration are correlated, but not identical. Sulfate concentration increases by more than 10 $\mu g/m^3$ from the southern part of NCP to central China and from most of the eastern part of SCB to the YRD region. Sulfate concentration increases by more than 20 $\mu g/m^3$ in SCB and up to more than 50 $\mu g/m^3$ in the central region, by 20-30 $\mu g/m^3$ in the YRD central region, and by 5-20 $\mu g/m^3$ in the PRD region.

https://doi.org/10.5194/egusphere-2023-521
Preprint. Discussion started: 24 March 2023

In summary, comparing the contribution of cloud chemistry in the whole December with the pollution maturity stage of 19-21, it shows that cloud chemistry in heavy pollution weather for SO_2 depletion and sulfate increase is mainly concentrated in the central-eastern part of China, and the four major pollution regions are also more obvious. However, SO_2 consumption and sulfate increase are not consistent, which is not only influenced by the local SO_2 concentration, but also by the cloud amount. Therefore, for SCB, which is less polluted and has much more clouds than NCP, the impact of cloud chemistry on sulfate and its precursor SO_2 is always the most significant in the SCB, both during heavy pollution and averaged over the whole December.

Exploring details into the pollution episode, it is found that the cloud chemistry influence is mainly on SCB and YRD at 21:00 LST on Dec. 20. The sulfate concentration increases (RT(sulfate)) by about 20-100 μg/m^3 in most parts of SCB, and the highest is about 150-225 μg/m^3 in its southwest (Fig. 8a). The increase is about 10-40 μg/m^3 in most parts of YRD, and the highest increase can reach 40-100 μg/m^3 in the southeast near Hangzhou Bay. At 21st 17:00 LST, it shows that the pollution episode has moved eastward and the cloud chemistry process has a stronger impact on NCP than that of the previous time (Fig. 8b). The increase center is located in Shandong Province, with up to 100-225 μg/m^3, and with about 10-60 μg/m^3 in most of NCP. In PRD, it has been influenced the least by the cloud process with sulfate concentration increase of 10-40 μg/m^3. At 22nd 12 LST, although the episode has gradually dissipated, it still had an impact on SCB and YRD with sulfate increase about 10-40 μg/m^3 in most of these four regions (Fig. 8c).

Above all, the contribution of cloud chemistry to surface sulfate during this pollution process is the highest in the SCB, followed by the NCP and YRD, with maximum concentration increases of 225 μg/m^3, 100 μg/m^3, and 40 μg/m^3, respectively, and sulfate increases of 10-40 μg/m^3 in most regions of these three areas.

Further analysis of the simulation characteristics of cloud chemistry on all the regions during the pollution maturity stage, i.e., the cloud process from Dec. 19 to 21 (Table 6), and the whole month of December (Table 7), is investigated. Compared with CCLD, R of SO2 in CLD increases by 0.6, 0.14, and 0.1 in YRD, SCB, and NCP, respectively, and the overestimation in NCP and PRD has been corrected during the pollution episode. R also increases by 0.1, 0.03 and 0.04 in YRD, SCB and NCP for the whole December, respectively.

For the performance of $PM_{2.5}$ of CLD, it decreases the underestimation in NCP and SCB with decreasing NMB and Rs remain almost the same with that of CCLD in the four pollution regions during the pollution episode and the whole December. There are little difference between the statistics results of R, NMB and RMSE with some positive improve for underestimation in NCP and SCB. R improves by 0.1 and NMB with cloud chemistry decreases from 39.25 % to 13.75 %. Moreover, the statistical results of all stations (SUM in Table 8) shows that the NMB of SO_2 decreased from 39.25% to

https://doi.org/10.5194/egusphere-2023-521
Preprint. Discussion started: 24 March 2023

13.75% and the NMB of sulfate increased from -40.75% to -31.62% during the pollution period after the addition of cloud chemistry simulation, so the simulation bias of both SO_2 and sulfate decreased during the pollution period.

305

3.3 Site evaluation of cloud chemistry

Representative sites of Beijing, Nanjing, Guangzhou and Chengdu at NCP, YRD, PRD and SCB are selected to quantify the impact of cloud chemistry during the pollution episode. The net depletion ratio of SO_2 column concentration ($RT(SO_2)$) during cloud chemistry is shown in Figure 9. It is found that SO_2 column concentration reduction maintained mostly a high
310 value of over 6 0%, even to 80 % sometimes, in Chengdu from 16th to 21st. In Nanjing, the SO_2 level is reduced by about 20-50 % during the time from 17th to 19th and up to 80 % from 20th to 21st when the episode matures there. The changes of SO_2 in these two cities are consistent with the changes in cloud and liquid cloud water content distributions during the pollution period in Figure 3. The SO_2 reduction in Beijing and Guangzhou is consistently maintained at around 40% during the time from 17th to 21th. The lower oxidative transformation is related to the lower liquid water content in Beijing, while in
315 Guangzhou it is attributed to the combination of low pollution levels and low cloud water content. Figure 3 shows that Chengdu maintained abundant water vapor conditions from 17th to 21st, and so does Nanjing from 20th to 21st. However, the ambient water vapor content is quite low in Guangzhou and Beijing throughout the process, so the SO_2 oxidation is much lower than that of Chengdu and Nanjing. In conclusion, the cloud chemistry process can lead to SO_2 column concentration consumption share of more than 60 % when cloud water content is abundant, which is also consistent with the observations
320 of Mount Tai by Li (2020).

The impact of cloud chemistry on surface SO_2 and sulfate in four sites are also shown in Figure 10. The overall trend shows that the peak and valley regions of surface SO_2 consumption and sulfate increase are coincident. The cloud chemical processes make the surface SO_2 oxidation vary greatly between cities in different regions (Fig. 10a). From the 19th to the 21st, the percentage of surface SO_2 consumption can reach more than 90% in Chengdu and Nanjing, while it is below 30% in
325 Beijing and Guangzhou, and does not reach 40% until the 22nd. Although the percentage of surface SO_2 consumption varies greatly, the increase in the percentage of sulfate does not vary so much between cities. From 16th to 22nd, the increase in surface sulfate in the four cities ranges from 60-95 % (Figure 10b), and the sulfate increase rate interval contains the results summarized by Turnock et al. (2019).

Figure 11 is the variation of vertical profiles of sulfate increase by cloud chemistry at the four times at 12:00 LST on 20
330 Dec., at 04:00 LST on 21 Dec., at 04:00 and 12:00 LST on 22 Dec. in Beijing, Nanjing, Chengdu and Guangzhou. It shows

https://doi.org/10.5194/egusphere-2023-521
Preprint. Discussion started: 24 March 2023

that the sulfate produced by cloud chemistry during this pollution process is concentrated mostly below 5 km in the troposphere, especially under 2 km. Again, less sulfate has been produced in Beijing in vertical than that of others by cloud chemistry.

4. Summary and conclusions

The cloud chemistry mechanism in WRF/CUACE has been assessed by using the in-situ cloud chemistry observations of SO_2, O_3, and H_2O_2 from Mount Tai in June-July 2015 and 2018. The results show that the mechanism well captures the cloud processes for the oxidation of SO_2, reducing SO_2 by more than 80 % during the cloudy phase of heavy pollution, which is in good agreement with the observations.

The cloud chemistry contributions to the changes of SO_2 and sulfate in NCP, YRD, PRD and SCB regions are assessed by WRF/CUACE. During the pollution episode from 19 to 21, all four pollution areas are significantly affected by cloud chemistry, with SCB being the most obvious, with surface SO_2 reduction averaging up to 1-3 ppb and reaching 3-10 ppb in the high value areas, and surface sulfate increasing 10-30 $\mu g/m^3$ on average, with a maximum of more than 70 $\mu g/m^3$. Most areas in NCP, YRD and PRD had an average SO_2 reduction of 0.5-3 ppb and sulfate increase of 5-30 $\mu g/m^3$. Meanwhile, the Beijing area of NCP had the least impact among the four regions. Although the average impact of cloud chemistry is much weaker in the NCP with less water vapor there in December, the contribution of the southern part of NCP during heavy pollution time is still significant and cannot be ignored. In PRD, the contribution of cloud chemistry is weaker than other regions due to lighter pollution, although there are lots of clouds with abounded liquid water there. In addition, surface sulfate increases by 60-95 % in Beijing, Nanjing, Chengdu and Guangzhou in December during heavy pollution, similar to that of previous studies (Faloona 2009; Turnock et al., 2019). Above all, the average contribution of cloud chemistry during the pollution period is significantly greater than that for all December. Vertically, the results of the pollution process for the 2016 winter heavy pollution episode showed that the cloud chemistry influence is mainly in the middle and lower troposphere below 2 km for four representative cities. Generally, the cloud chemistry improved the model performance by reducing the SO_2 overestimates and enhancing the correlations with observations for both SO_2 and sulfate.

This paper has been focused on the cloud chemical mechanism evaluation, and assessed the contribution of cloud chemistry to SO_2 and sulfate changes. In the future, more mechanisms should be added to improve the cloud chemistry mechanism in CUACE to more accurately simulate SO_2 and sulfate and other aerosol components such as nitrate, ammonium, carbonate, and organic aerosols.

https://doi.org/10.5194/egusphere-2023-521
Preprint. Discussion started: 24 March 2023

Code/data availability

All source code and data can be accessed by contacting the corresponding authors Sunling Gong (gongsl@cma.gov.cn).

Authors contribution

CZ and SG put forward the ideas and formulated overarching research goals. JL carried them out and wrote the manuscript with suggestions from all authors. LZ and JZ participated in the scientific interpretation and discussion. JC was assisted with data acquisition and processing. All authors contributed to the discussion and improvement of the manuscript.

Competing interests

The authors declare that they have no conflict of interest.

Financial support

This research has been supported by the National Key Project of the Ministry of Science and Technology of China (2022YFC3701205); CMA Innovation Development Project (CXFZ2021J023).

https://doi.org/10.5194/egusphere-2023-521
Preprint. Discussion started: 24 March 2023

References

Alexander, B., Park, R. J., Jacob, D. J., and Gong, S.: Transition metal-catalyzed oxidation of atmospheric sulfur: Global implications for the sulfur budget, Journal of Geophysical Research, 114, https://doi.org/10.1029/2008jd010486, 2009.

Buchard, V., da Silva, A. M., Colarco, P., Krotkov, N., Dickerson, R. R., Stehr, J. W., Mount, G., Spinei, E., Arkinson, H. L., and He, H.: Evaluation of GEOS-5 sulfur dioxide simulations during the Frostburg, MD 2010 field campaign, Atmos. Chem. Phys., 14, 1929-1941, https://doi.org/10.5194/acp-14-1929-2014, 2014.

Binkowski, F. S., and Roselle, S. J.: Models - 3 Community Multiscale Air Quality (CMAQ) model aerosol component 1. Model description, Journal of Geophysical Research: Atmospheres, 108, https://doi.org/10.1029/2001jd001409, 2003.

Caffrey, P., Hoppel, W., Frick, G., Pasternack, L., Fitzgerald, J., Hegg, D., Gao, S., Leaitch, R., Shantz, N., Albrechcinski, T., and Ambrusko, J.: In-cloud oxidation of SO_2 by O_3 and H_2O_2: Cloud chamber measurements and modeling of particle growth, Journal of Geophysical Research: Atmospheres, 106, 27587-27601, https://doi.org/10.1029/2000jd900844, 2001.

Chang, J. S., Brost, R. A., Isaksen, I. S. A., Madronich, S., Middleton, P., Stockwell, W. R., and Walcek, C. J.: A three-dimensional eulerian acid deposition model physical concepts and formulation, journal of geophysical research, 92, 14,681-614,700, https://doi.org/10.1029/jd092id12p14681, 1987.

Chapman, E. G., Gustafson, W. I., Easter, R. C., Barnard, J. C., and Fast, J. D.: Coupling aerosol-cloud-radiative processes in the WRF-Chem model: Investigating the radiative impact of elevated point sources, Atmos. Chem. Phys., 9, 945 - 964, https://doi.org/10.5194/acp-9-945-2009, 2009.

Charlson, R., J., Schwartz, and S., E.: Climate forcing by anthropogenic aerosols, Science, 255, 423-423, https://doi.org/10.1126/science.255.5043.423, 1992.

Emery, C., Tai, E., and Yarwood, G.: Enhanced meteorological modeling and performance evaluation for two Texas ozone episodes, 2001.

Cheng, Y., Zheng, G., Wei, C., Mu, Q., Zheng, B., Wang, Z., Gao, M., Zhang, Q., He, K., and Carmichael, G.: Reactive nitrogen chemistry in aerosol water as asource of sulfate during haze events in China, Science Advances, https://doi.org/10.1126/sciadv.1601530, 2016.

Dovrou, E., Rivera-Rios, J. C., Bates, K. H., and Keutsch, F. N.: Sulfate Formation via Cloud Processing from Isoprene Hydroxyl Hydroperoxides (ISOPOOH), Environ Sci Technol, 53, 12476-12484, https://doi.org/10.1021/acs.est.9b04645, 2019.

Ervens, B.: Modeling the Processing of Aerosol and Trace Gases in Clouds and Fogs, Chemical Reviews, 115, 4157-4198, https://doi.org/10.1021/cr5005887, 2015.

https://doi.org/10.5194/egusphere-2023-521
Preprint. Discussion started: 24 March 2023

Faloona, I.: Sulfur processing in the marine atmospheric boundary layer: A review and critical assessment of modeling uncertainties. Atmospheric Environment, 43(18), 2841-2854, https://doi.org/10.1016/j.atmosenv.2009.02.043, 2009.

Faloona, I., Conley, S. A., Blomquist, B., Clarke, A. D., Kapustin, V., Howell, S., Lenschow, D. H., and Bandy, A. R.: Sulfur dioxide in the tropical marine boundary layer: dry deposition and heterogeneous oxidation observed during the Pacific Atmospheric Sulfur Experiment, Journal of Atmospheric Chemistry, 63, 13-32, https://doi.org/10.1007/s10874-010-9155-0, 2010.

Gao, M., Carmichael, G. R., Wang, Y., Ji, D., Liu, Z., and Wang, Z.: Improving simulations of sulfate aerosols during winter haze over Northern China: the impacts of heterogeneous oxidation by NO_2, Frontiers of Environmental Science & Engineering, 10, 11, https://doi.org/10.1007/s11783-016-0878-2, 2016.

Ge, W., Liu, J., Yi, K., Xu, J., Zhang, Y., Hu, X., Ma, J., Wang, X., Wan, Y., Hu, J., Zhang, Z., Wang, X., and Tao, S.: Influence of atmospheric in-cloud aqueous-phase chemistry on global simulation of SO_2 in CESM2, Atmos. Chem. Phys., https://doi.org/10.5194/acp-2021-406, 2021.

Georgiou, G. K., Christoudias, T., Proestos, Y., Kushta, J., Hadjinicolaou, P., and Lelieveld, J.: Air quality modelling in the summer over the eastern Mediterranean using WRF-Chem: chemistry and aerosol mechanism intercomparison, Atmos. Chem. Phys., 18, 1555-1571, https://doi.org/10.5194/acp-18-1555-2018, 2018.

Gen, M.; Zhang, R.; Huang, D. D.; Li, Y.; Chan, C. K.: Heterogeneous SO_2 Oxidation in Sulfate Formation by Photolysis of Particulate Nitrate, Environ. Sci. Technol, 6 (2), 86−91, https://doi.org/10.1021/acs.estlett.8b00681, 2019a.

Gen, M., Zhang, R., Huang, D. D., Li, Y., and Chan, C. K.: Heterogeneous Oxidation of SO(2) in Sulfate Production during Nitrate Photolysis at 300 nm: Effect of pH, Relative Humidity, Irradiation Intensity, and the Presence of Organic Compounds, Environ Sci Technol, 53, 8757-8766, https://doi.org/10.1021/acs.est.9b01623, 2019b.

Gong, S., and Zhang, X.: CUACE/Dust – an integrated system of observation and modeling systems for operational dust forecasting in Asia, Atmospheric Chemistry and Physics, 8, 2333-2340, https://doi.org/10.5194/acp-8-2333-2008, 2008.

Gong, S. L., Barrie, L. A., Blanchet, J.-P., von Salzen, K., Lohmann, U., Lesins, G., Spacek, L., Zhang, L. M., Girard, E., Lin, H., Leaitch, R., Leighton, H., Chylek, P., and Huang, P.: Canadian Aerosol Module: A size-segregated simulation of atmospheric aerosol processes for climate and air quality models 1. Module development, Journal of Geophysical Research, 108, https://doi.org/10.1029/2001jd002002, 2003.

Guo, J., Wang, Y., Shen, X., Wang, Z., Lee, T., Wang, X., Li, P., Sun, M., Jeffrey, L., Collett, J., Wang, W., and Wang, T.: Characterization of cloud water chemistry at Mount Tai, China: Seasonal variation, anthropogenic impact, and cloud processing, Atmospheric Environment, 60, 467-476, https://doi.org/10.1016/j.atmosenv.2012.07.016, 2012.

https://doi.org/10.5194/egusphere-2023-521
Preprint. Discussion started: 24 March 2023

Guo, S., Hu, M., Zamora, M. L., Peng, J., Shang, D., Zheng, J., Du, Z., Wu, Z., Shao, M., Zeng, L., Molina, M. J., and Zhang, R.: Elucidating severe urban haze formation in China, Proc Natl Acad Sci U S A, 111, 17373-17378, https://doi.org/10.1073/pnas.1419604111, 2014.

Harris, E., Sinha, B., van Pinxteren, D., Tilgner, A., Fomba, K. W., Schneider, J., Roth, A., Gnauk, T., Fahlbusch, B., Mertes, S., Lee, T., Collett, J., Foley, S., Borrmann, S., Hoppe, P., and Herrmann, H.: Enhanced role of transition metal ion catalysis during in-cloud oxidation of SO_2, Science, 340, 727-730, https://doi.org/10.1126/science.1230911, 2013.

He, J., Zhang, Y., Glotfelty, T., He, R., Bennartz, R., Rausch, J., and Sartelet, K.: Decadal simulation and comprehensive evaluation of CESM/CAM5.1 with advanced chemistry, aerosol microphysics, and aerosol-cloud interactions, Journal of Advances in Modeling Earth Systems, 7, 110-141, https://doi.org/10.1002/2014ms000360, 2015.

Hung, H. M., Hsu, M. N., and Hoffmann, M. R.: Quantification of SO_2 Oxidation on Interfacial Surfaces of Acidic Micro-Droplets: Implication for Ambient Sulfate Formation, Environ Sci Technol, 52, 9079-9086, https://doi.org/10.1021/acs.est.8b01391, 2018.

Kotarba, A. Z.: Calibration of global MODIS cloud amount using CALIOP cloud profiles, Atmospheric Measurement Techniques, 13, 4995-5012, https://doi.org/10.5194/amt-13-4995-2020, 2020.

IIbusuki, T., and Takeuchi, K.: Sulfur dioxide oxidation by oxygen catalyzed by mixtures of manganese(II) and iron(III) in aqueous solutions at environmental reaction conditions, Atmospheric Environment, 21, 1555-1560, https://doi.org/10.1016/0004-6981(87)90317-9, 1987.

Leighton, H. G., and Ivanova, I. T.: Aerosol–Cloud Interactions in a Mesoscale Model. Part I: Sensitivity to Activation and Collision–Coalescence, Journal of the Atmospheric Sciences, 65, 289-308, https://doi.org/10.1175/2007jas2207.1, 2008.

Lelieveld, Jos, Heintzenberg, and Jost: Sulfate cooling effect on climate through in-cloud oxidation of anthropogenic SO_2, Science, https://doi.org/10.1126/science.258.5079.117, 1992.

Li, J. R.: Microphysical Characteristics and S(IV) Multiphase Chemical Reaction Mechanism of Orographic Clouds, Ph.D. thesis, Fudan University, 127pp, 2020.

Li, J., Wang, X., Chen, J., Zhu, C., Li, W., Li, C., Liu, L., Xu, C., Wen, L., Xue, L., Wang, W., Ding, A., and Herrmann, H.: Chemical composition and droplet size distribution of cloud at the summit of Mount Tai, China, Atmos. Chem. Phys., 17, 9885-9896, https://doi.org/10.5194/acp-17-9885-2017, 2017.

Li, J., Zhu, C., Chen, H., Fu, H., Xiao, H., Wang, X., Herrmann, H., and Chen, J.: A More Important Role for the Ozone - S(IV) Oxidation Pathway Due to Decreasing Acidity in Clouds, Journal of Geophysical Research: Atmospheres, 125, https://doi.org/10.1029/2020jd033220, 2020a.

https://doi.org/10.5194/egusphere-2023-521
Preprint. Discussion started: 24 March 2023

Li, J., Zhu, C., Chen, H., Zhao, D., Xue, L., Wang, X., Li, H., Liu, P., Liu, J., Zhang, C., Mu, Y., Zhang, W., Zhang, L., Herrmann, H., Li, K., Liu, M., and Chen, J.: The evolution of cloud and aerosol microphysics at the summit of Mt. Tai, China, Atmos. Chem. Phys., 20, 13735-13751, https://doi.org/10.5194/acp-20-13735-2020, 2020b.

Li, M., Liu, H., Geng, G., Hong, C., Liu, F., Song, Y., Tong, D., Zheng, B., Cui, H., Man, H., Zhang, Q., and He, K.: Anthropogenic emission inventories in China: a review, Natl. Sci. Rev., 4, 834-866, https://doi.org/10.1093/nsr/nwx150, 2017.

Liu, S. C., McKeen, S. A., Hsie, E.-Y., Lin, X., Kelly, K. K., Bradshaw, J. D., Sandholm, S. T., Browell, E. V., Gregory, G. L., Sachse, G. W., Bandy, A. R., Thornton, D. C., Blake, D. R., Rowland, F. S., Newell, R., Heikes, B. G., Singh, H., and R. W. Talbot: Model study of tropospheric trace species distributions during PEM-WEST A, J. Geophys. Res, 101, https://doi.org/0148-0227/96/95JD-02277505.00, 1996.

Li, P. F.: Fog Water Chemistry and Fog-Haze Transformation in Shanghai, Fudan University, Ph.D. thesis, 145pp.

Liu, T., Chan, A. W. H., and Abbatt, J. P. D.: Multiphase Oxidation of Sulfur Dioxide in Aerosol Particles: Implications for Sulfate Formation in Polluted Environments, Environ Sci Technol, 55, 4227-4242, https://doi.org/10.1021/acs.est.0c06496, 2021.

Maahs, H. G.: Kinetics and Mechanism of the Oxidation of S(IV) by Ozone in Aqueous Solution With Particular Reference to SO_2 Conversion in Nonurban Tropospheric Clouds, journal of geophysical research oceans, 88, 10721-10732, https://doi.org/10.1029/JC088iC15p10721, 1983.

Martin, G. M., D. W. Johnson, and A. Spice, The measurement and parameterization of effective radius in warm stratocumulus cloud, J. Atmos. Sci., 51, 1823-1842, https://doi.org/10.1175/1520-0469(1994)051<1823:TMAPOE>2.0.CO;2, 1994.

Martin, L. R., and Good, T. W.: Catalyzed oxidation of sulfur dioxide in solution: The iron-manganese synergism, Atmospheric Environment, 25, 2395-2399, https://doi.org/10.1016/0960-1686(91)90113-L, 1991.

Menut, L., Bessagnet, B., Khvorostyanov, D., Beekmann, M., Colette, A., Coll, I., Curci, G., Foret, G., Hodzic, A., Mailler, S., Meleux, F., Monge, J. L., Pison, I., Turquety, S., Valari, M., Vautard, R., and Vivanco, M. G.: Regional atmospheric composition modeling with CHIMERE, Geoscientific Model Development, 6, 981–1028, https://doi.org/10.5194/gmdd-6-203-2013, 2013.

Molina: Air Quality in the Mexico Megacity: An Integrated Assessment, Alliance for Global Sustainability Bookseries, https://doi.org/10.1007/978-94-010-0454-1, 2002.

Park, R. J., and Jacob, D. J.: Sources of carbonaceous aerosols over the United States and implications for natural visibility, Journal of Geophysical Research, 108, https://doi.org/10.1029/2002jd003190, 2003.

https://doi.org/10.5194/egusphere-2023-521
Preprint. Discussion started: 24 March 2023

Pye, H. O. T., Nenes, A., Alexander, B., Ault, A. P., Barth, M. C., Clegg, S. L., Jr., J. L. C., Fahey, K. M., Hennigan, C. J., Herrmann, H., Kanakidou, M., Kelly, J. T., Ku, I.-T., McNeill, V. F., Riemer, N., Schaefer, T., Shi, G., Tilgner, A., Walker, J. T., Wang, T., Weber, R., Xing, J., Zaveri, R. A., and Zuend, a. A.: Havala O. T. Pye The acidity of atmospheric particles and clouds, Atmos. Chem. Phys., 20, 4809 – 4888, https://doi.org/10.5194/acp-20-4809-2020, 2020.

Ramanathan, V., Crutzen, P. J., Kiehl, J. T., and Rosenfeld, D.: Aerosols, climate, and the hydrological cycle, Science, 294, 2119-2124, 10.1126/science.1064034, 2001.

Ravishankara, A. R.: Heterogeneous and Multiphase Chemistry in the Troposphere, Science, 276, 1058-1065, https://doi.org/10.1126/science.276.5315.1058, 1997.

Ren, Y., Ding, A., Wang, T., Shen, X., Guo, J., Zhang, J., Wang, Y., Xu, P., Wang, X., and Gao, J.: Measurement of gas-phase total peroxides at the summit of Mount Tai in China, Atmospheric Environment, 43, 1702-1711, https://doi.org/10.1016/j.atmosenv.2008.12.020, 2009.

Sha, T., Ma, X., Jia, H., Tian, R., Chang, Y., Cao, F., and Zhang, Y.: Aerosol chemical component: Simulations with WRF-Chem and comparison with observations in Nanjing, Atmospheric Environment, 218, https://doi.org/10.1016/j.atmosenv.2019.116982, 2019.

Shen, X., Lee, T., Guo, J., Wang, X., Li, P., Xu, P., Wang, Y., Ren, Y., Wang, W., Wang, T., Li, Y., Carn, S. A., and Collett, J. L.: Aqueous phase sulfate production in clouds in eastern China, Atmospheric Environment, 62, 502-511, https://doi.org/10.1016/j.atmosenv.2012.07.079, 2012.

Shimadera, H., Kondo, A., Shrestha, K. L., Kaga, A., and Inoue, Y.: Annual sulfur deposition through fog, wet and dry deposition in the Kinki Region of Japan - ScienceDirect, Atmospheric Environment, 45, 6299-6308, https://doi.org/10.1016/j.atmosenv.2011.08.055, 2011.

Sielski, J., Kazirod-Wolski, K., Jozwiak, M. A., and Jozwiak, M.: The influence of air pollution by PM2.5, PM10 and associated heavy metals on the parameters of out-of-hospital cardiac arrest, Sci Total Environ, 788, 147541, https://doi.org/10.1016/j.scitotenv.2021.147541, 2021.

Song, S., Nenes, A., Gao, M., Zhang, Y., Liu, P., Shao, J., Ye, D., Xu, W., Lei, L., Sun, Y., Liu, B., Wang, S., and McElroy, M. B.: Thermodynamic Modeling Suggests Declines in Water Uptake and Acidity of Inorganic Aerosols in Beijing Winter Haze Events during 2014/2015–2018/2019, Environmental Science & Technology Letters, 6, 752-760, htttps://doi.org/10.1021/acs.estlett.9b00621, 2019.

Terrenoire, E., Bessagnet, B., Rouïl, L., Tognet, F., Pirovano, G., Létinois, L., Beauchamp, M., Colette, A., Thunis, P., Amann, M., and Menut, L.: High-resolution air quality simulation over Europe with the chemistry transport model CHIMERE,

https://doi.org/10.5194/egusphere-2023-521
Preprint. Discussion started: 24 March 2023

Geoscientific Model Development, 8, 21-42, https://doi.org/10.5194/gmd-8-21-2015, 2015.

Tie, X.: Assessment of the global impact of aerosols on tropospheric oxidants, Journal of Geophysical Research, 110, https://doi.org/10.1029/2004jd005359, 2005.

Tremblay, A., and Leighton, H.: A Three-Dimensional Cloud Chemistry Model, Journal of Climate & Applied Meteorology, 25, 652-671, https://doi.org/10.1016/1352-2310(96)00063-5, 1986.

Turnock, S. T., Mann, G. W., Woodhouse, M. T., Dalvi, M., O'Connor, F. M., Carslaw, K. S., and Sprackle, D. V.: The Impact of Changes in Cloud Water pH on Aerosol Radiative Forcing, Geophysical Research Letters, 46, 4039 – 4048, https://doi.org/10.1029/2019GL082067, 2019.

Twomey: Aerosols, clouds and radiation, Atmospheric Environment.part A.general Topics, 25, 2435-2442, https://doi.org/10.1016/0960-1686(91)90159-5, 1991.

Twomey, S. A., Piepgrass, M., and Wolfe, T. L.: An assessment of the impact of pollution on the global cloud albedo, Tellus B: Chemical and Physical Meteorology, 36B, 356-366, https://doi.org/10.1111/j.1600-0889.1984.tb00254.x, 1984.

von Salzen, K., Leighton, H. G., Ariya, P. A., Barrie, L. A., Gong, S. L., Blanchet, J. P., Spacek, L., Lohmann, U., and Kleinman, L. I.: Sensitivity of sulphate aerosol size distributions and CCN concentrations over North America to SOx emissions and H2O2 concentrations, Journal of Geophysical Research: Atmospheres, 105, 9741-9765, https://doi.org/10.1029/2000jd900027, 2000.

Wang, G., Zhang, R., Gomez, M. E., Yang, L., Levy Zamora, M., Hu, M., Lin, Y., Peng, J., Guo, S., Meng, J., Li, J., Cheng, C., Hu, T., Ren, Y., Wang, Y., Gao, J., Cao, J., An, Z., Zhou, W., Li, G., Wang, J., Tian, P., Marrero-Ortiz, W., Secrest, J., Du, Z., Zheng, J., Shang, D., Zeng, L., Shao, M., Wang, W., Huang, Y., Wang, Y., Zhu, Y., Li, Y., Hu, J., Pan, B., Cai, L., Cheng, Y., Ji, Y., Zhang, F., Rosenfeld, D., Liss, P. S., Duce, R. A., Kolb, C. E., and Molina, M. J.: Persistent sulfate formation from London Fog to Chinese haze, Proc Natl Acad Sci U S A, 113, 13630-13635, https://doi.org/10.1073/pnas.1616540113, 2016.

Wang, H., Shi, G. Y., Zhang, X. Y., Gong, S. L., Tan, S. C., Chen, B., Che, H. Z., and Li, T.: Mesoscale modelling study of the interactions between aerosols and PBL meteorology during a haze episode in China Jing – Jin – Ji and its near surrounding region – Part 2: Aerosols' radiative feedback effects, Atmos. Chem. Phys.,15,6(2015-03-23), 14, 3277-3287, https://doi.org/10.5194/acp-15-3257-2015, 2015.

Wang, J., Li, J., Ye, J., Zhao, J., Wu, Y., Hu, J., Liu, D., Nie, D., Shen, F., Huang, X., Huang, D. D., Ji, D., Sun, X., Xu, W., Guo, J., Song, S., Qin, Y., Liu, P., Turner, J. R., Lee, H. C., Hwang, S., Liao, H., Martin, S. T., Zhang, Q., Chen, M., Sun, Y., Ge, X., and Jacob, D. J.: Fast sulfate formation from oxidation of SO_2 by NO_2 and HONO observed in Beijing haze, Nature Communications, 11, 10.1038/s41467-020-16683-x, 2020.

https://doi.org/10.5194/egusphere-2023-521
Preprint. Discussion started: 24 March 2023

Wang, S., Zhou, S., Tao, Y., Tsui, W. G., Ye, J., Yu, J. Z., Murphy, J. G., McNeill, V. F., Abbatt, J. P. D., and Chan, A. W. H.: Organic Peroxides and Sulfur Dioxide in Aerosol: Source of Particulate Sulfate, Environ Sci Technol, 53, 10695-10704, https://doi.org/10.1021/acs.est.9b02591, 2019.

Wei, Y., Chen, X., Chen, H., Li, J., Wang, Z., Yang, W., Ge, B., Du, H., Hao, J., Wang, W., Li, J., Sun, Y., and Huang, H.: IAP-AACM v1.0: a global to regional evaluation of the atmospheric chemistry model in CAS-ESM, Atmos. Chem. Phys., 19, 8269-8296, https://doi.org/10.5194/acp-19-8269-2019, 2019.

Xie, Y., Dai, H., Zhang, Y., Wu, Y., Hanaoka, T., and Masui, T.: Comparison of health and economic impacts of $PM_{2.5}$ and ozone pollution in China, Environ Int, 130, 104881, https://doi.org/10.1016/j.envint.2019.05.075, 2019.

Yao, S., Wang, Q., Zhang, J., and Zhang, R.: Characteristics of Aerosol and Effect of Aerosol-Radiation-Feedback in Handan, an Industrialized and Polluted City in China in Haze Episodes, Atmosphere, 12, 670, https://doi.org/10.3390/atmos12060670, 2021.

Yao, M., Zhao, Y., Hu, M., Huang, D., Wang, Y., Yu, J. Z., and Yan, N.: Multiphase Reactions between Secondary Organic Aerosol and Sulfur Dioxide: Kinetics and Contributions to Sulfate Formation and Aerosol Aging, Environmental Science & Technology Letters, 6, 768-774, htttps://doi.org/10.1021/acs.estlett.9b00657, 2019.

Ye, C., Xue, C., Zhang, C., Ma, Z., Liu, P., Zhang, Y., Liu, C., Zhao, X., Zhang, W., He, X., Song, Y., Liu, J., Wang, W., Sui, B., Cui, R., Yang, X., Mei, R., Chen, J., and Mu, Y.: Atmospheric Hydrogen Peroxide H_2O_2 at the Foot and Summit of Mt Tai Variations Sources, Journal of Geophysical Research: Atmospheres, 126, https://doi.org/10.1029/2020JD033975, 2021.

Ye, J., Abbatt, J. P. D., and Chan, A. W. H.: Novel pathway of SO_2 oxidation in the atmosphere: reactions with monoterpene ozonolysis intermediates and secondary organic aerosol, Atmos. Chem. Phys., 18, 5549-5565, htttps://doi.org/10.5194/acp-18-5549-2018, 2018.

Yuan, D. M., Ma, X. H.: The severe haze process in 16 – 21 December 2016 and associated atmospheric circulation anomalies [J]. Climatic and Environmental Research (in Chinese), 22 (6): 757 – 764, https://doi.org/10.3878/j.issn.1006-9585.2017.17029, 2017.

Zhang, L., Gong, S., Zhao, T. L., Zhou, C. H., and Zhang, X. Y.: Development of WRF/CUACE v1.0 model and its preliminary application in simulating air quality in China, Geoscientific Model Development, https://doi.org/10.5194/gmd-14-703-2021, 2021.

Zhang, X. Y., Wang, Y. Q., Niu, T., Zhang, X. C., Gong, S. L., Zhang, Y. M., and Sun, J. Y.: Atmospheric aerosol compositions in China: spatial/temporal variability, chemical signature, regional haze distribution and comparisons with global aerosols, Atmos. Chem. Phys., 12, 779-799, https://doi.org/10.5194/acp-12-779-2012, 2012.

https://doi.org/10.5194/egusphere-2023-521
Preprint. Discussion started: 24 March 2023

Zheng, B., Tong, D., Li, M., Liu, F., Hong, C., Geng, G., Li, H., Li, X., Peng, L., Qi, J., Yan, L., Zhang, Y., Zhao, H., Zheng, Y., He, K., and Zhang, Q.: Trends in China's anthropogenic emissions since 2010 as the consequence of clean air actions, Atmos. Chem. Phys., 18, 14095-14111, https://doi.org/10.5194/acp-18-14095-2018, 2018.

Zheng, B., Zhang, Q., Zhang, Y., He, K. B., Wang, K., Zheng, G. J., Duan, F. K., Ma, Y. L., and Kimoto, T.: Heterogeneous chemistry: a mechanism missing in current models to explain secondary inorganic aerosol formation during the January 2013 haze episode in North China, Atmos. Chem. Phys., 14, 2031-2049, https://doi.org/10.5194/acp-15-2031-2015, 2015.

Zhou, C. H., Gong, S., Zhang, X. Y., Liu, H. L., Xue, M., Cao, G. L., An, X. Q., and Che, H. Z.: Towards the improvements of simulating the chemical and optical properties of Chinese aerosols using an online coupled model - CUACE/Aero, Chemical and physical and meteorology, https://doi.org/10.3402/tellusb.v64i0.18965, 2012.

Zhou, C. H., Zhang, X. Y., Gong, S., Wang, Y. Q., and Xue, M.: Improving aerosol interaction with clouds and precipitation in a regional chemical weather modeling system, Atmospheric Chemistry and Physics, 16, 145-160, https://doi.org/10.5194/acp-16-145-2016, 2016.

Zhou Y., Gong S., Zhou C., Zhang L., He J., Wang Y., Ji D., Feng J., Mo J., Ke H..: A new parameterization of uptake coefficients for heterogeneous reactions on multi-component atmospheric aerosols, Science of the Total Environment, 781, https://doi.org/10.1016/j.scitotenv.2021.146372, 2021.

https://doi.org/10.5194/egusphere-2023-521
Preprint. Discussion started: 24 March 2023

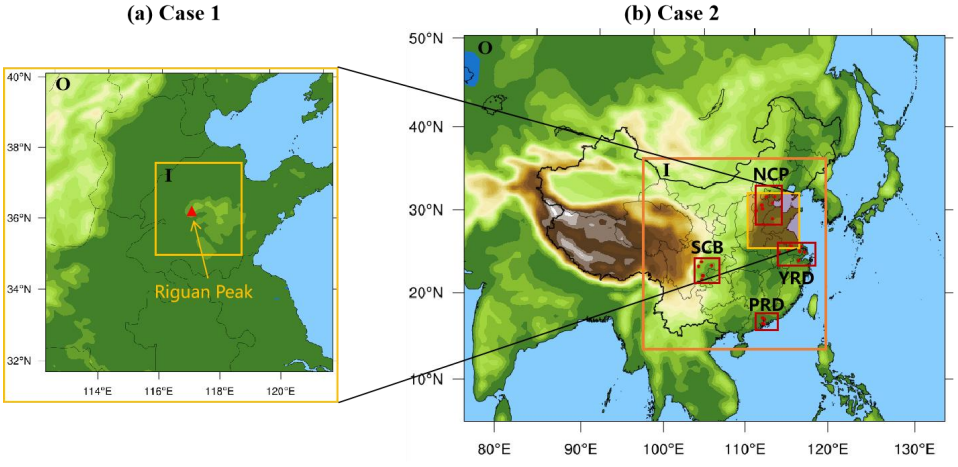

Figure 1. Model nesting domains and target regions: (a) domain for the Case 1. The red triangle is the Mount Tai site, (b) nesting domains for regional assessment for Case 2. Red dots are where the surface observations of air pollutants are. The target four regions are NCP for the North China Plain, YRD for the Yangtze River Delta , PRD for the Pearl River Delta and SCB for the Sichuan Basin.

https://doi.org/10.5194/egusphere-2023-521
Preprint. Discussion started: 24 March 2023

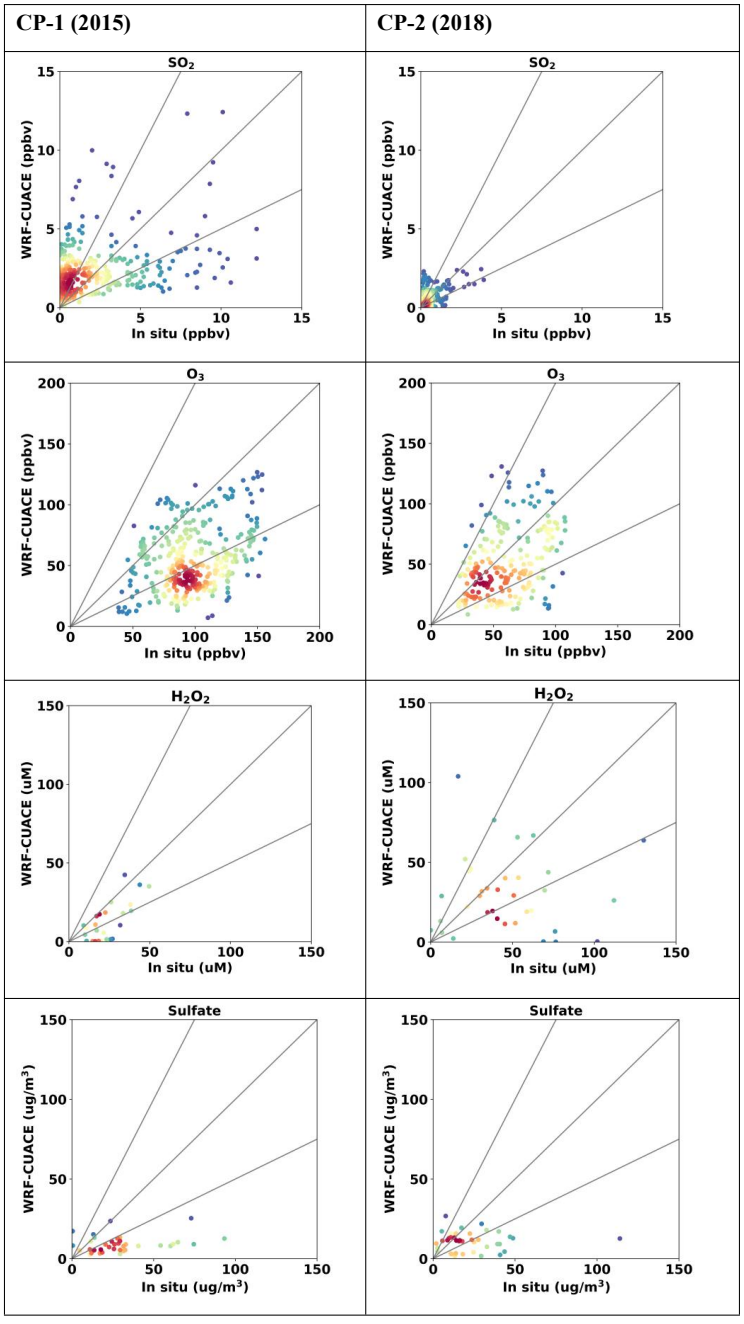

Figure 2. Scatter plots of hourly SO_2, O_3, H_2O_2 and sulfate concentrations between WRF/CUACE and in situ observations at Mount Tai.

https://doi.org/10.5194/egusphere-2023-521
Preprint. Discussion started: 24 March 2023

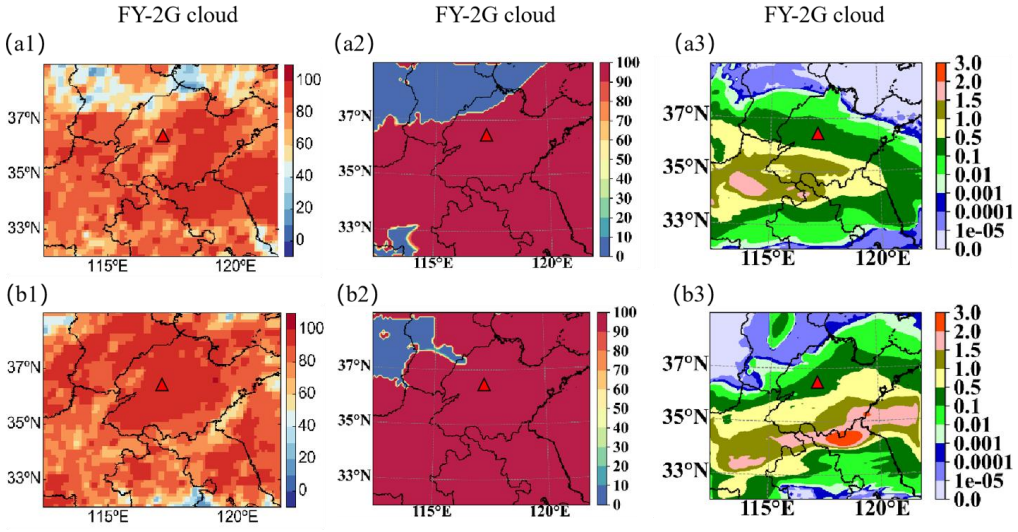

Figure 3. (a1, b1): the cloud image of FY2G, (a2, b2): the cloud fraction by WRF/CUACE. (a3, b3): the liquid water content by WRF/CUACE (Units: g m^{-2}). (a) is for 8:00 LST on 24 June, (b) is for 8:00 LST on 25 June.

https://doi.org/10.5194/egusphere-2023-521
Preprint. Discussion started: 24 March 2023

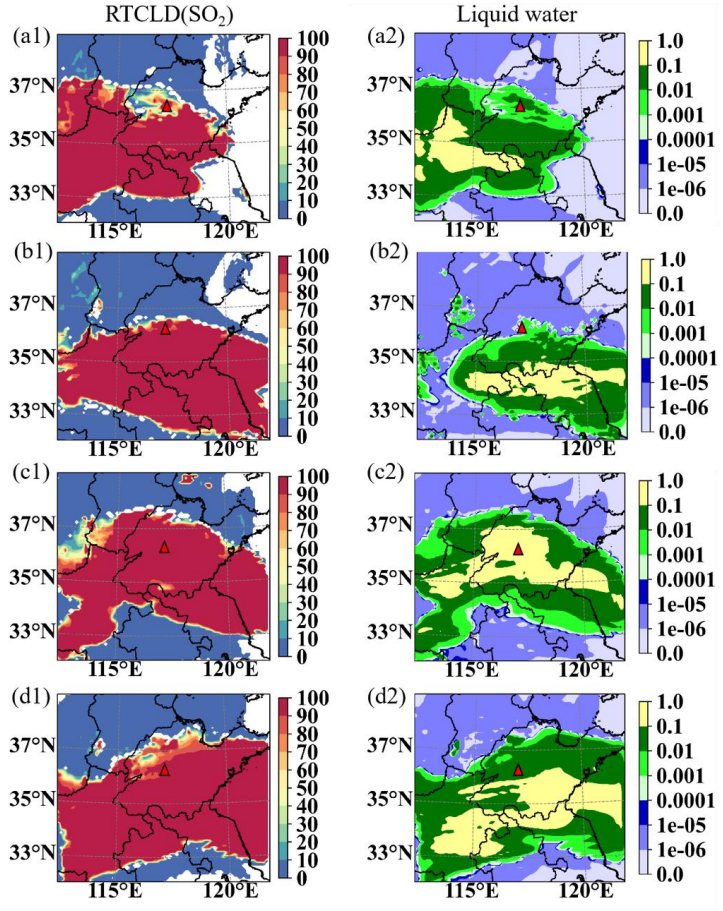

Figure 4. The percentage of SO_2 oxidized (a1, b1, c1 and d1) (%) and the liquid water content (a2, b2, c2 and d2) (g/kg) by WRF/CUACE, where (a) is for 2:00 LST on 24 June, (b) is for 8:00 LST on 24 June, (c) is for 2:00 LST on 25 June and (d) is for 8:00 LST on 25 June.

https://doi.org/10.5194/egusphere-2023-521
Preprint. Discussion started: 24 March 2023

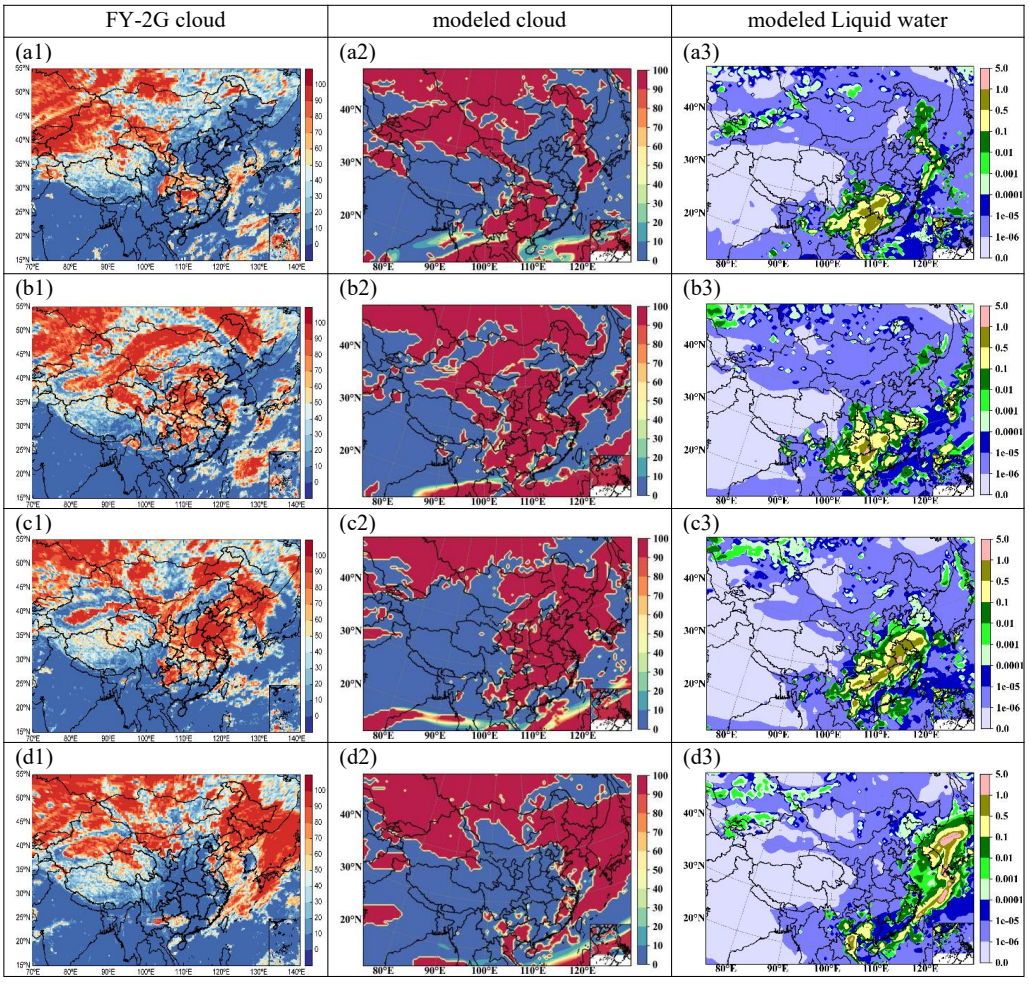

Figure 5. (a1, b1, c1, d1): the cloud image of FY-2G (%); (a2, b2, c2, d2): the column cloud of WRF/CUACE (%); (a3, b3, c3, d3): the liquid water content of WRF/CUACE (g/m^2). (a) is for 8:00 LST on 19 Dec., (b) is for 8:00 LST on 20 Dec., (c) is for 8:00 LST on 21 Dec., and (d) is for 8:00 LST on 22 Dec.

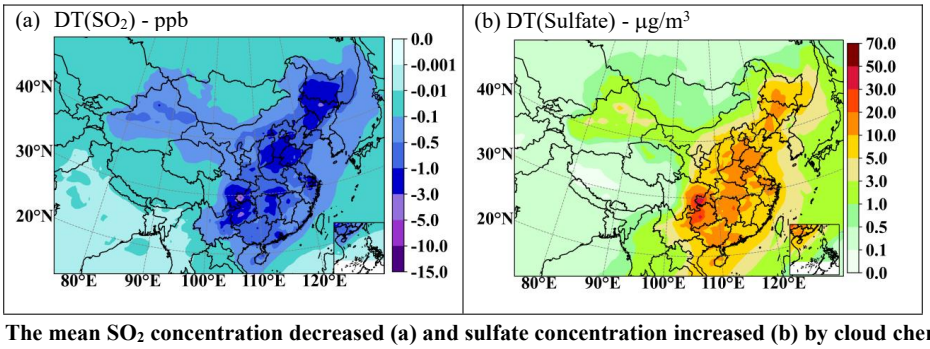

Figure 6. The mean SO_2 concentration decreased (a) and sulfate concentration increased (b) by cloud chemistry in Dec. 2016.

https://doi.org/10.5194/egusphere-2023-521
Preprint. Discussion started: 24 March 2023

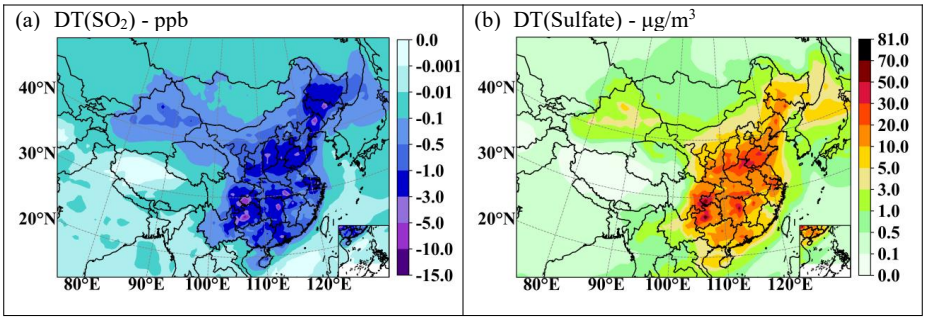

Figure 7. The mean SO_2 concentration decreased (a) and sulfate concentration increased (b) by cloud chemistry from 19-21 Dec., 2016.

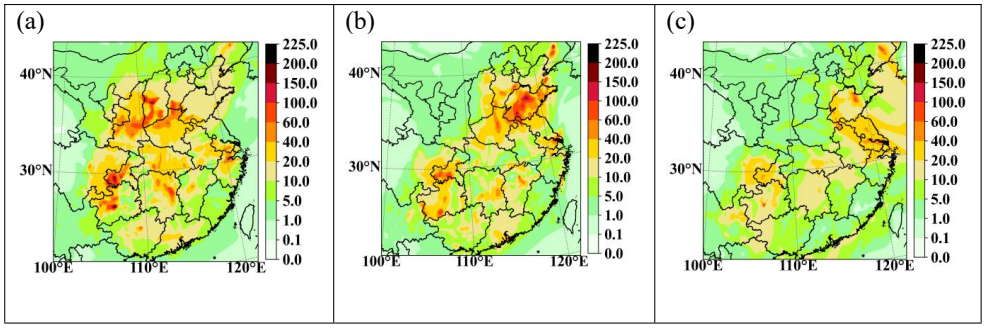

Figure 8. The differences in surface sulfate concentrations between with and without cloud chemistry at 21:00 on 20 Dec. (a), at 17:00 on 21 Dec. (b), and at 12:00 on 22 Dec. (c) (μg/m³).

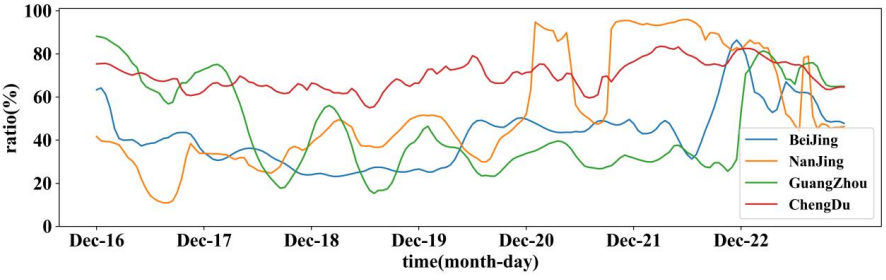

Figure 9. The percentage of SO_2 column concentration reduced due to oxidation in cloud chemistry.

https://doi.org/10.5194/egusphere-2023-521
Preprint. Discussion started: 24 March 2023

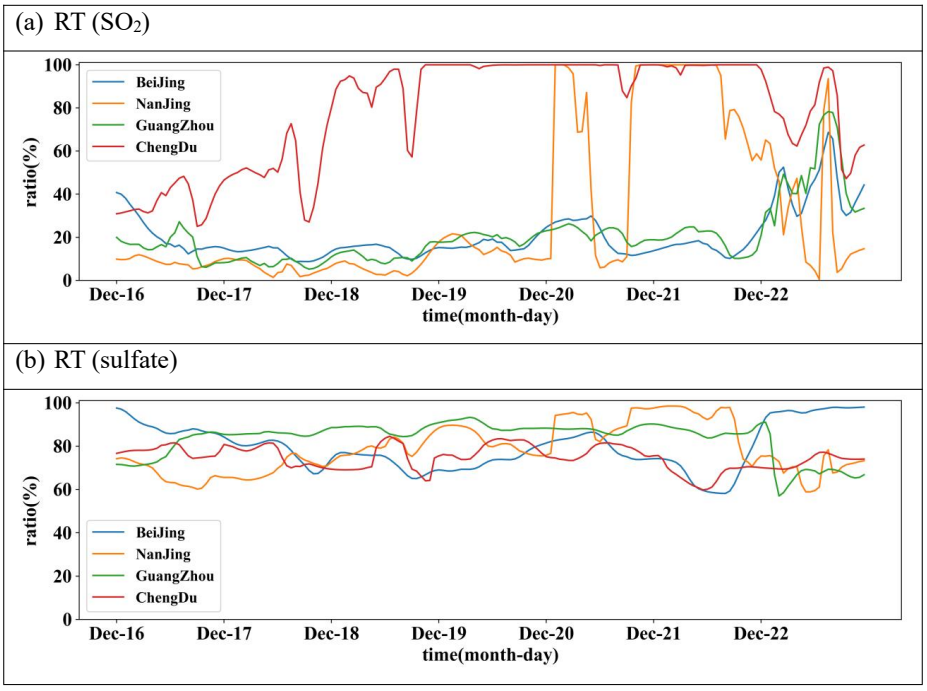

Figure 10. The percentage of surface SO_2 reduced (a) and the surface sulfate increased (b) influenced by cloud chemistry.

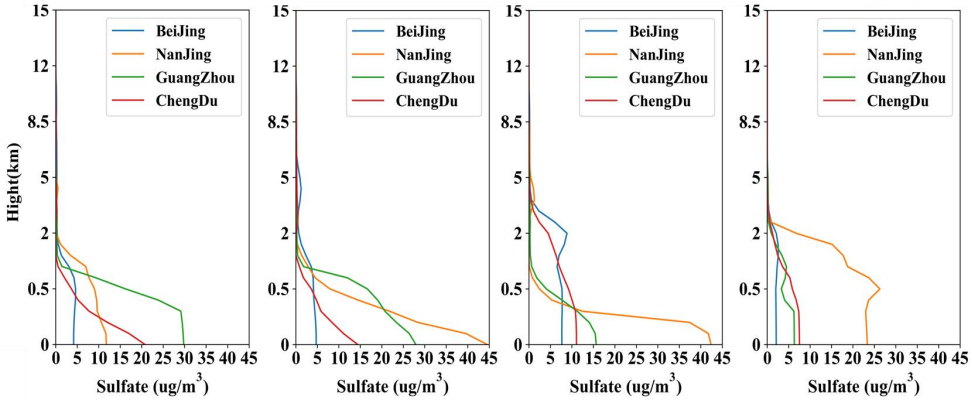

Figure 11. Vertical profiles of sulfate concentration difference DT at 12:00 on 20 Dec., at 21:00 on 20 Dec., at 17:00 on 21 Dec., and at 12:00 on 22 Dec.

https://doi.org/10.5194/egusphere-2023-521
Preprint. Discussion started: 24 March 2023

Table 1. Equilibrium Constants for the Parameterization of the Cloud Chemistry in CUACE.

Equilibrium Relation	Constant Expression	Equilibrium Constant K(298)	a	Unit
$SO_2(g)+H_2O(aq)\leftrightarrow SO_2(aq)$	$K_{HS}=\frac{[SO_2(aq)]}{[SO_2(g)]}$	1.23	3120	$\frac{M}{\text{atm}}$
$SO_2(aq)\leftrightarrow H^+ + HSO_3^-$	$K_{1S}=\frac{[H^+][HSO_3^-]}{[SO_2(aq)]}$	1.7×10^{-2}	2090	M
$HSO_3^- \leftrightarrow H^+ + SO_3^{2-}$	$K_{2S}=\frac{[H^+][SO_3^{2-}]}{[HSO_3^-]}$	6.0×10^{-8}	1120	M
$O_3(g)+H_2O(aq)\leftrightarrow O_3(aq)$	$K_{HO}=\frac{[O_3(aq)]}{[O_3(g)]}$	1.15×10^{-2}	2560	$\frac{M}{\text{atm}}$
$H_2O_2(g)+H_2O(aq)\leftrightarrow H_2O_2(aq)$	$K_{HP}=\frac{[H_2O_2(aq)]}{[H_2O_2(g)]}$	9.7×10^{4}	6600	$\frac{M}{\text{atm}}$

Table 2. physics parameterization schemes in WRF.

Physical management	Parameterization	References
microphysics scheme	Lin	Lin et al. (1983)
shortwave radiation	Goddard	Chou and Suarez (1994)
longwave radiation	RRTM	Mlawer et al. (1997)
land surface scheme	Noah	Chen and Dudhia (2001)
boundary layer scheme	MYJ	Janjić (1994)
cumulus scheme	Grell-3D	Grell (1993)

Table 3. Statistics for SO_2, O_3, H_2O_2 and sulfate in cloud chemistry at Mount Tai site.

		Obs.	Mod		R	RAD(%)	NMB(%)
CP-1	SO_2(ppbv)	2.16	2.32	SO_2	0.34	-3.4	7.1
	O_3(ppbv)	97.79	55.27	O_3	0.33	27.8	-43.5
	H_2O_2(uM)	26.52	16.83	H_2O_2	0.78	22.4	-36.6
	Sulfate(μg/m^3)	31.68	9.20	Sulfate	0.32	55.0	-71.0
CP-2	SO_2(ppbv)	0.56	0.63	SO_2	0.47	-6.1	12.9
	O_3(ppbv)	60.68	50.97	O_3	0.40	8.7	-16.0
	H_2O_2(uM)	46.92	32.36	H_2O_2	0.06	18.4	-29.6
	Sulfate(μg/m^3)	28.08	11.40	Sulfate	0.54	42.2	-59.4

https://doi.org/10.5194/egusphere-2023-521
Preprint. Discussion started: 24 March 2023

Table 4. Statistical metrics for meteorology in NCP, YRD, PRD and SCB for Dec. 16-21 and the whole Dec. in 2016.

		Obs.		Mod			R		NMB(%)	
		16-21	Dec.	16-21	Dec.		16-21	Dec.	16-21	Dec.
NCP	T2(℃)	0.99	1.11	2.83	2.05	T2	0.70	0.84	187.3	84.9
	RH2(%)	78.83	68.31	52.30	48.75	RH2	0.54	0.64	-33.7	-28.6
	WS10(m/s)	1.47	1.69	1.67	2.16	WS10	0.49	0.54	14.1	27.5
YRD	T2(℃)	9.24	7.99	9.51	8.40	T2	0.94	0.96	2.9	5.1
	RH2(%)	79.22	75.62	73.81	72.98	RH2	0.86	0.85	-6.8	-3.5
	WS10(m/s)	2.16	2.27	2.78	2.99	WS10	0.74	0.76	28.7	31.9
PRD	T2(℃)	18.31	17.27	18.98	17.93	T2	0.93	0.92	3.6	3.8
	RH2(%)	72.19	70.43	64.31	65.35	RH2	0.76	0.68	-10.9	-7.2
	WS10(m/s)	1.78	2.36	2.02	3.24	WS10	0.67	0.72	13.6	37.1
SCB	T2(℃)	10.18	9.70	10.46	9.99	T2	0.74	0.75	2.8	3.1
	RH2(%)	81.63	79.92	74.09	71.26	RH2	0.66	0.60	-9.2	-10.8
	WS10(m/s)	1.09	1.27	1.63	1.92	WS10	0.49	0.36	49.1	50.5

Table 5. Statistical metrics for hourly SO_2, O_3 and $PM_{2.5}$ in NCP, YRD, PRD and SCB for Dec. 16-21 and the whole Dec. in 2016.

		Obs.(μg/m^3)		Mod(μg/m^3)		R		NMB(%)	
		16-21	Dec.	16-21	Dec.	16-21	Dec.	16-21	Dec.
NCP	SO_2	41.99	61.45	49.98	39.99	0.60	0.48	46.3	-15.6
	O_3	8.75	7.41	7.42	10.89	0.47	0.60	-15.3	-32.4
	$PM_{2.5}$	351.33	182.08	194.75	110.79	0.30	0.62	-48.2	-35.7
YRD	SO_2	21.81	16.30	15.82	14.90	0.61	0.45	-25.3	-32.8
	O_3	31.25	14.37	9.25	22.11	0.33	0.68	-54.0	-45.5
	$PM_{2.5}$	70.26	82.90	119.14	84.23	0.70	0.73	18.0	19.3
PRD	SO_2	13.64	24.01	24.02	16.98	0.32	0.39	76.1	11.9
	O_3	45.74	56.27	56.51	57.36	0.84	0.80	23.0	13.9
	$PM_{2.5}$	55.66	83.56	83.78	77.54	0.84	0.39	50.1	51.5
SCB	SO_2	19.98	10.03	12.43	8.80	0.49	0.19	-49.8	-47.4
	O_3	21.97	49.01	45.27	54.19	0.20	0.47	123.1	97.4
	$PM_{2.5}$	135.56	90.99	117.03	70.99	0.27	0.28	-32.9	-29.1

https://doi.org/10.5194/egusphere-2023-521
Preprint. Discussion started: 24 March 2023

Table 6. Statistical metrics for hourly SO_2 and $PM_{2.5}$ in NCP, YRD, PRD and SCB for Dec. 19-21, respectively.

19-21 Dec.		SO_2				$PM_{2.5}$(μg/m^3)			
		NCP	YRD	PRD	SCB	NCP	YRD	PRD	SCB
Obs.(μg/m^3)		41.99	21.81	13.64	19.98	351.33	70.26	55.66	135.56
Mod (μg/m^3)	CLD	49.98	15.82	24.02	12.43	194.75	119.14	83.78	117.03
	CCLD	65.61	25.68	30.81	15.84	166.60	63.82	77.00	72.55
R	CLD	0.60	0.61	0.32	0.49	0.30	0.70	0.84	0.27
	CCLD	0.61	0.55	0.31	0.34	0.31	0.77	0.83	0.30
NMB(%)	CLD	46.4	-25.3	76.1	-49.8	-48.2	18.0	50.1	-32.9
	CCLD	56.3	17.7	125.9	-20.7	-52.6	-9.2	38.3	-46.5

Table 7. Statistical metrics for hourly SO_2 and $PM_{2.5}$ in NCP, YRD, PRD and SCB for Dec., respectively.

Dec.		SO_2				$PM_{2.5}$			
		NCP	YRD	PRD	SCB	NCP	YRD	PRD	SCB
Obs(μg/m^3)		47.36	22.17	15.18	16.72	172.18	70.59	51.18	100.11
Mod (μg/m^3)	CLD	39.99	14.90	16.98	8.80	110.79	84.23	77.54	70.99
	CCLD	44.68	19.51	20.71	13.59	93.58	71.81	70.11	55.91
R	CLD	0.48	0.45	0.39	0.19	0.62	0.73	0.39	0.28
	CCLD	0.50	0.35	0.34	0.16	0.65	0.77	0.38	0.33
NMB(%)	CLD	-15.6	-32.8	11.9	-47.4	-35.7	19.3	51.5	-29.1
	CCLD	-5.7	-12.0	36.4	-18.8	-45.7	1.7	37.0	-44.2

Table 8. Statistical metrics for hourly SO_2 , O_3 and $PM_{2.5}$ in all sellected sites for Dec. 16-21 and the whole Dec..

SUM		19-21		Dec.	
		SO_2	$PM_{2.5}$	SO_2	$PM_{2.5}$
Obs.(μg/m^3)		25.68	167.95	27.01	32.19
Mod (μg/m^3)	CLD	29.21	114.85	21.35	87.56
	CCLD	35.75	99.51	25.85	74.05
R	CLD	0.66	0.67	0.64	0.56
	CCLD	0.65	0.70	0.63	0.57
NMB (%)	CLD	13.8	-31.6	-21.0	-16.3
	CCLD	39.3	-40.8	-4.3	-29.2